JOURNAL OF GEOPHYSICAL RESEARCH, VOL. 102, NO. D24, PAGES 28,805–28,816, DECEMBER 26, 1997

Moss and soil contributions to the annual net carbon flux of a maturing boreal forest

J. W. Harden,[1] K. P. O'Neill,[1] S. E. Trumbore,[2] H. Veldhuis,[3] and B. J. Stocks[4]

Abstract. We used input and decomposition data from ^{14}C studies of soils to determine rates of vertical accumulation of moss combined with carbon storage inventories on a sequence of burns to model how carbon accumulates in soils and moss after a stand-killing fire. We used soil drainage—moss associations and soil drainage maps of the old black spruce (OBS) site at the BOREAS northern study area (NSA) to areally weight the contributions of each moderately well drained, feathermoss areas; poorly drained sphagnum—feathermoss areas; and very poorly drained brown moss areas to the carbon storage and flux at the OBS NSA site. On this very old (117 years) complex of black spruce, sphagnum bog veneer, and fen systems we conclude that these systems are likely sequestering 0.01–0.03 kg C m^{-2} yr^{-1} at OBS-NSA today. Soil drainage in boreal forests near Thompson, Manitoba, controls carbon storage and flux by controlling moss input and decomposition rates and by controlling through fire the amount and quality of carbon left after burning. On poorly drained soils rich in sphagnum moss, net accumulation and long-term storage of carbon is higher than on better drained soils colonized by feathermosses. The carbon flux of these contrasting ecosystems is best characterized by soil drainage class and stand age, where stands recently burned are net sources of CO_2, and maturing stands become increasingly stronger sinks of atmospheric CO_2. This approach to measuring carbon storage and flux presents a method of scaling to larger areas using soil drainage, moss cover, and stand age information.

Introduction

Boreal ecosystems and their influence on global carbon and energy cycles are receiving increasing attention from the global change community for a number of reasons [*Bonan et al.*, 1992; *Tans et al.*, 1990; *Ciais et al.*, 1995]. First, the soils of the boreal region contain significant carbon reservoirs that have accumulated over several thousands of years; perhaps more importantly, these soils are still active sinks for terrestrial carbon. Short growing seasons, cold temperatures, and high moisture contents limit decomposition of organic matter, resulting in thick accumulations of carbon-rich material on the forest floor [*Harden et al.*, 1992; *Billings*, 1987]. Moreover, unlike northern wetlands that respond to climate shifts only after decades, the boreal forest is more sensitive to changes in temperature and moisture and may begin to respond after only a matter of years [*Bonan and Hayden*, 1990; *Bonan and Chapin*, 1995]. Under a warming scenario, such as that documented for recent decades in this region [*Beltrami and Mareschal*, 1991], the fate of this stored soil carbon and its effect on global climate is of growing concern. Second, the complex interactions of climate and CO_2 suggest that northern latitudes may be a likely candidate for a terrestrial CO_2 feedback to anthropogenic CO_2 rise, specifically in the form of a "missing or undefined CO_2 sink." The argument for a missing CO_2 sink is not new (although only recently focused on northern latitudes), yet it continues to evade a mechanistic understanding from the research community [*Tans et al.*, 1990; *Ciais et al.*, 1995; *Francey et al.*, 1995; *Houghton*, 1993]. Third, discontinuous permafrost, such as that found in the northern study area (NSA) of the Boreal Ecosystem-Atmosphere Study (BOREAS), is rich in peatlands [*Zoltai*, 1993] and highly sensitive to changes in mean air temperature, potentially altering energy and water feedbacks to the carbon, climate, and energy cycles [*Lachenbruch*, 1994; *Thie*, 1974; *Brown*, 1983].

Unlike most soils of temperate and tropical systems, many soils of northern black spruce forests have a highly developed organic-rich LFH (litter-fibric-humic) or peaty horizon that overlies the mineral soil. The organic portion of the soil profile may be divided into two distinct components with different physical and chemical characteristics. The top part is composed of living and recently dead mosses that are relatively undecomposed. This layer is characterized by low bulk density and high percent carbon (%C) values similar to those in living mosses. This shallow layer may burn completely or partially in a stand-killing fire and thickens with time as moss regrows in the decades following fire. Deeper in the soil profile, decomposition acts on residual charred and decomposed material that has accumulated over the millennia during postglacial time. As this deep organic material becomes more decomposed, bulk density increases, %C decreases, and hydraulic conductivity becomes lower. Because the processes and rates of carbon accumulation and decomposition vary significantly among shallow and deeper horizons, we have quantified them separately. In this paper, the term "shallow moss layer" refers to both live and dead moss in various stages of decomposition. In layers where material is no longer distinguishable as "moss" we use the terms "decomposed organics" or "deep organic layers."

Two of the primary controls on carbon storage in northern

[1]U.S. Geological Survey, Menlo Park, California.
[2]Earth System Science, University of California, Irvine.
[3]Agriculture Canada, Winnipeg, Manitoba.
[4]Forestry Canada, Sault Sainte Marie, Ontario.

Paper number 97JD02237.
0148-0227/97/97JD-02237$09.00

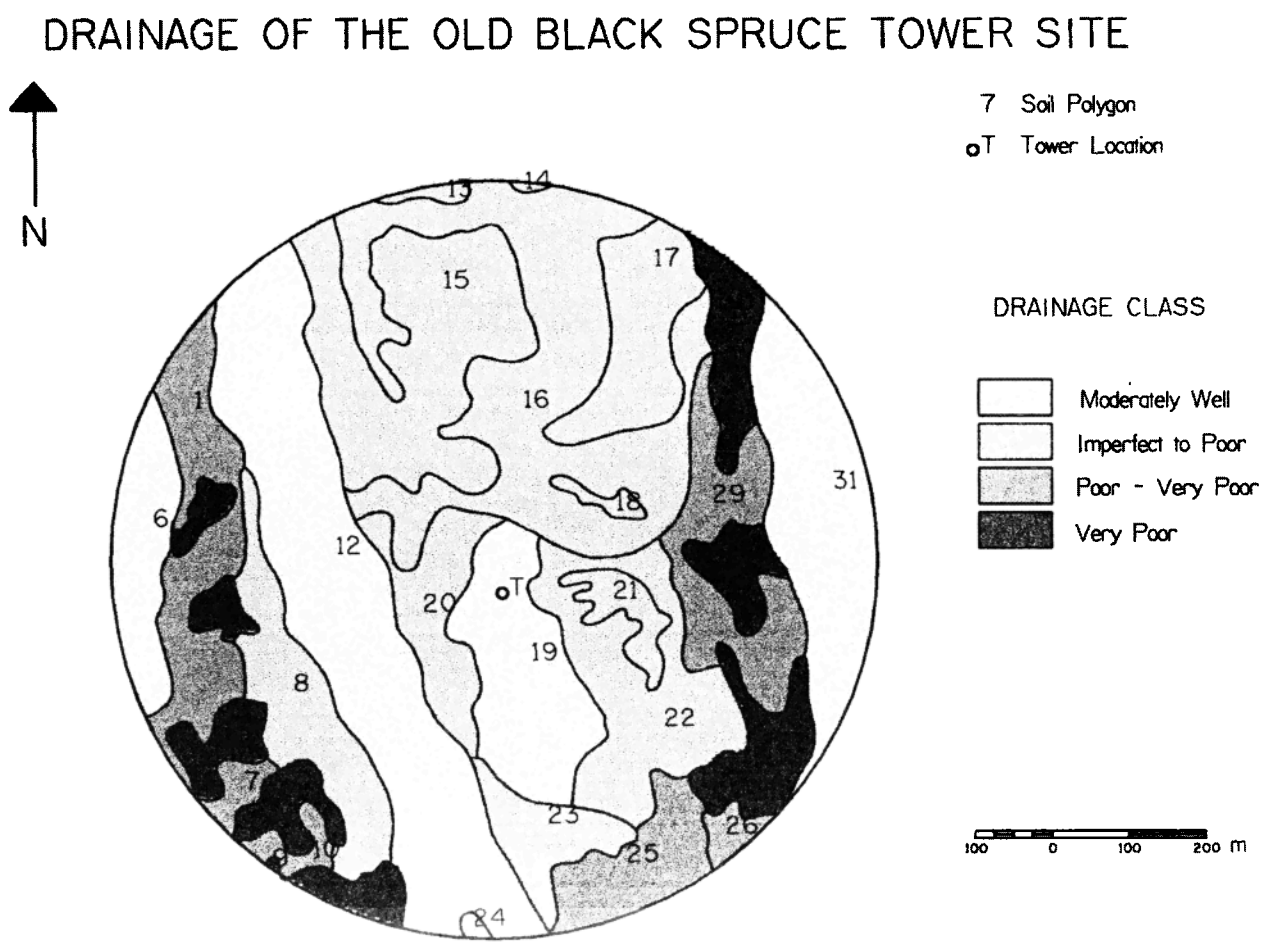

Figure 1. Soil drainage and moss-cover map of the old black spruce (northern study area) of BOREAS: 1, moderately well drained areas are feathermoss dominated and cover 24% of the map; 2, imperfect to poorly drained feathermoss/sphagnum areas cover 15% of the map; 3, poorly drained, sphagnum/feathermoss bog veneers cover 30% of the map; 4, very poor to poorly drained sphagnum/brown moss areas cover 16% of the map. Very poorly drained brown moss fen areas cover 10% of the map.

soils are moisture content and soil drainage. Soils that are poorly drained and remain wet through the summer have slower rates of decomposition and may not burn completely. Productivity in poorly drained soils is similar to or exceeds (in fens) that of well-drained uplands. Together, these factors result in greater carbon storage and higher rates of carbon accumulation in poorly drained soils.

Fire exerts a major control on moss layers in boreal forest soils [*Racine*, 1981]. During a fire event, moss is burned off of well-drained or dry areas, reducing the amount of the forest floor that is covered by moss. That moss which survives the fire tends to be restricted to moist or depressional portions of the landscape. As the system recovers from the fire, moss will move from these localized areas and begin to recolonize the forest floor by sporing or by lateral expansion.

Our main objective in this paper is to estimate the present-day contributions of soil and moss to the carbon balance in a mature forest (NSA-OBS). In order to achieve this goal, we examine how carbon fluxes from various soil types have changed over the most recent fire cycle (~120 years) by (1) mapping soil drainage patterns and moss association under the OBS flux tower (Figure 1), (2) determining carbon inputs to the organic soil from plant production for each soil drainage-moss association, (3) determining rates of carbon loss through decomposition in shallow moss and deeper organic layers for each drainage-moss association, (4) estimating the effects of fire and drainage on spatial distribution of regrowing moss. Estimates of net primary production (NPP) for mosses, decomposition rates (k), and net ecosystem exchange (NEP) are constructed from measurements of carbon accumulation on a time sequence of fire scars (for the two better drained soil types) and depth sequences for peat profiles (for wetlands). These carbon fluxes are then scaled to the OBS-NSA tower site according to soil drainage and moss cover type based on a 1–5000 soils map. Three classifications are used in scaling: (1) moderately well drained soils dominated by feathermoss, (2) poorly drained veneer bog and sphagnum hummocks, and (3) very poorly drained fen sites that are related to collapse of permafrost. Soil carbon flux is then estimated for the evolving complex of soil types as they regenerated from fire over the last century. Flux contributions to the OBS-NSA tower are estimated by applying this spatial and temporal model of soil carbon dynamics based on 117 years since the last stand-killing fire.

Methods of Sampling and Analysis

Soil and vegetation samples were collected from three soil-vegetation units that were identified in field studies over three summers from 1993 to 1996.

Dated sequence of moss layers. For estimating input (net primary production) and decomposition rates of mosses, layers of moss and organics were sampled in fine increments (2 to 10 cm thicknesses), and moss, leaves, seeds, and other datable components were separated for ^{14}C dating [*Trumbore and Harden*, this issue]. Carbon inventories were determined from volumetric samples collected from boxes of known volume, usually 14 cm × 18 cm × layer thickness, with moisture and bulk density determined as described below. For the very poorly drained wetlands, such as the BOREAS tower fen, a copper pipe was inserted into the upper meter of moss and peat through which we circulated liquid N_2. Organic material was frozen in place around the copper pipe, allowing us to extract frozen "cores" of material. These cores were immediately divided into 4 cm depth intervals; within each of these intervals, a cube of measured volume was removed using a reciprocating saw or serrated knife. Gravimetric moisture was tracked independently by collecting a separate suite of samples. A set of air-dry splits was milled and analyzed for C and N according to methods described below. A separate set of splits was examined under the microscope and individual moss leaves removed for ^{14}C analysis [*Trumbore and Harden*, this issue; *O'Neill et al.*, 1997a, b].

Age sequence of burn scars. An age sequence of burn scars and controls was located in black spruce stands adjacent to the BOREAS NSA supersite; burn scars range from 2 to 117 years in age. At each burn site, samples were collected along transects across a range of soil drainage classes.

Moss and organic soil layers were described at 10–12 locations along each transect and sampled for bulk density, organic carbon, and moisture content. At each sampling point, we attempted to locate the depth at which the most recent fire event had occurred (as evidenced by a pronounced char layer) and use that as a common basal depth for separating shallow, postburn layers from deeper, preburn layers. All moss and organic materials above this char layer were considered to have accumulated since the last fire disturbance.

Representative volumetric samples were collected for each moss and soil horizon using either an aluminum 14 cm × 18 cm, three-sided box, open to the pit face for sampling or by a 4 cm diameter aluminum core in conjunction with a gravimetric channel-sample for the horizon. Samples for a given layer or horizon were collected within the box from top to basal depths of each horizon (channel samples) and used for chemical analysis and moisture determination; in some cases the bulk density and chemical analyses were performed on the same sample, and moisture content was determined separately; in other cases, moisture and bulk density were determined on the same sample, and chemical analyses were performed separately. Rocks and organic matter >2 mm in diameter were removed and weighed prior to analysis. After saving a representative split for archive, the remainder of the sample was air dried. Moisture content of organic layers (>50% organic material by weight) was determined by 2-day weight loss in a 68°C oven; moisture content of inorganic materials was determined by 2-day weight loss in a 105°C oven. These data may be found in the BOREAS Information System (BORIS) data archives.

Total carbon content was measured on air-dry splits using a LECO total combustion analyzer or a FISONS NA-1500 combustion analyzer. An air-dry split was also acidified to determine organic carbon content; inorganic carbon was determined as the difference between organic and total carbon. Calcium carbonate was present only in some deeper mineral horizons, as a component of the Lake Agassiz sediments on which the soils have developed. Although carbon analysis was performed on an air-dry sample, results are reported on an oven-dry basis (grams carbon per grams oven dry soil *100). Some error is expected in this conversion as dried mosses will absorb atmospheric vapor; however, such errors are small compared to variations in field properties along the transects.

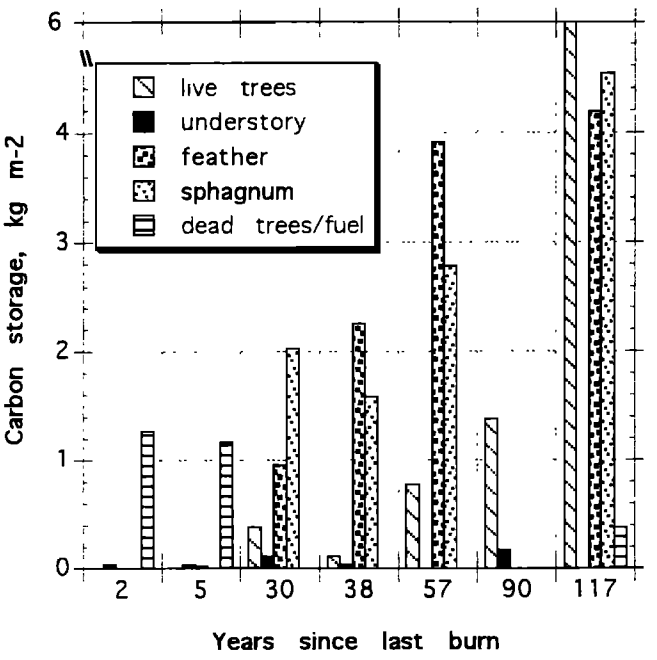

Figure 2. Biomass and organic matter measurements from transects at each burn. Tree biomass and fuel are from methods of *Stocks* [1989] for all but 117 years OBS site, for which data of S. T. Gower (personal communication, 1997; destructive sampling) are used. Understory data are from destructive sampling of 8–10 vegetation plots at each burn site. Moss data are from Table 1 and are based on soil excavations along the transect.

Samples were collected along burn transects for estimating carbon storage in biomass (trees and understory) and woody debris. Tree biomass was estimated from diameter breast height (DBH) measurements using relationships developed in Ontario for jack pine [*Walker and Stocks*, 1975; *Stocks*, 1980] and black spruce [*Stocks*, 1989] (Figure 2). Only trees and shrubs greater than 1.37 m (4.5 feet) tall were included in DBH data; those less than 1.37 m tall were included as an understory species and measured by harvesting material in 1 m^2 plots at five to eight sites along the transect. These samples were then dried at 68°C for 2 days to determine oven-dry biomass. Species and percent cover of moss and understory plants were also recorded at each sample location (data not shown).

The areal coverage of moss over the fire scar were collected as eye-ball estimates on the 6–8 m^2 plots harvested for understory along each transect.

Results and Model Development

For the soils represented by the burn sequence, trees and moss comprise roughly equal amounts of biomass in these boreal forest systems (Figure 2). Understory may play a critical role in shading recent burns and allowing moss and new trees to become established, but carbon storage in the understory is a minor amount compared to moss and trees.

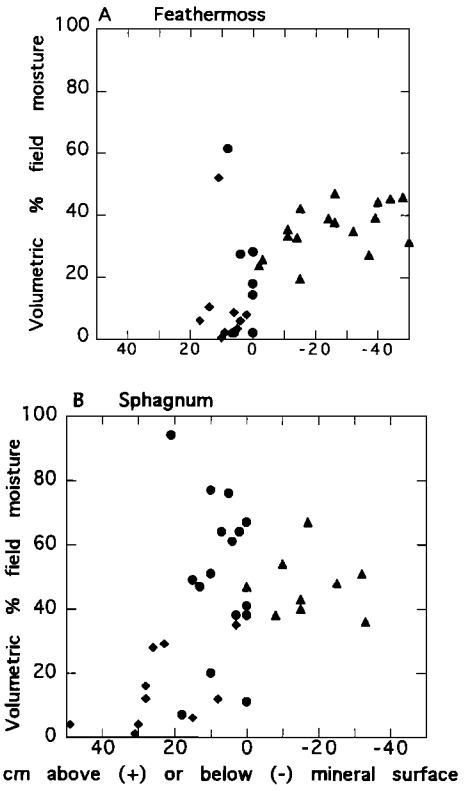

Figure 3. Percent moisture in field samples versus depth for profiles overlain by (a) feathermoss and (b) sphagnum. Moisture samples were collected destructively after 3 weeks of summer drought. Diamonds represent moss layers regrown since last fire; circles represent organic litter and peat layers; triangles represent mineral soil layers. Moisture is retained in sphagnum-covered soil, especially in organic peats overlying mineral soil.

Moss cover clearly changes over time, starting as low as 3% in recent burns of drier feathermoss areas. There was no significant increase in percent sphagnum cover with burn age, because sphagnum growth is more dependent upon drainage class than on time since fire, and drainage was not constant across all transects.

Burn age	5	30	38	57	80	117
% feathermoss cover	2.5	10	20	30	25	54
% sphagnum cover	...	2	33	2	43	40

C dynamics in shallow, postfire feathermoss covers. Feathermoss, composed mainly of *Pleurozium schreberi* and *Hylocomium splendens* (J. Bubier, personal communication, 1995), dominates those moderately well-drained sites that are covered by dense black spruce stands and underlain by permafrost (Figure 1); this unit represents 30% of the OBS soil map today. Feathermoss also occurs in combination with sphagnum and other mosses at sites that are imperfectly and poorly drained; as much as 30–50% of these soil units are covered in feathermoss today. During the summer these mosses typically dry throughout the thickness of the organic layer (Figure 3a); consequently, these sites generally burn deeply, resulting in considerable loss of decomposed organics. As a result, the carbon storage in feathermoss sites is lower than that of the wetter sphagnum sites, especially in organic layers (Figure 4). As the site recovers, feathermoss regrows over the area; thus both thickness of moss and areal coverage of moss increase over time since fire.

Because of their propensity to burn, areal coverage of feathermosses on recent burn scars is low, representing only 3% of the area based on species plots along transects of recent burns (Figure 5; data shown above). Coverage increases to 50% of the OBS map within 117 years following fire. Ultimately, however, areal coverage depends on local soil drainage, which is the reason for using the soil drainage maps at OBS for the fire-recovery model.

To model the changes in carbon storage and flux over time, we separated upward accumulation from lateral spread of moss, in which the upward accumulation is characterized by carbon inputs minus carbon loss by decomposition; the lateral spread of moss is characterized by percent areal coverage in the fire sequence.

The vertical accumulation of carbon in feathermoss was modeled from moss-layer studies of carbon inventory and age and is presented in detail by [*Trumbore and Harden*, this issue]; carbon inputs (I) and decomposition (k) are defined by the following equation:

$$dC/dt = I - kC \quad (1)$$

$$Ct = I/k(1 - \exp - kt) \quad (2)$$

where C is carbon mass in units of mass per area (kg C m^{-2}), t is time (years), I is input rate in mass per area per year (kg m^{-2} yr^{-1}), and k is a decomposition coefficient in units of

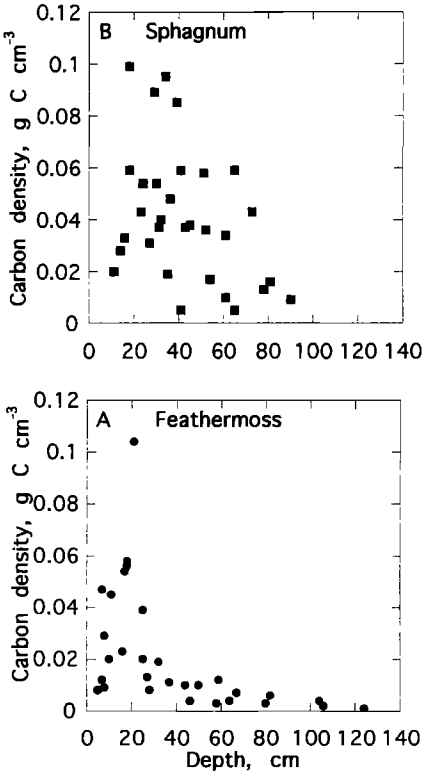

Figure 4. Carbon density of soil horizons as a function of depth for (a) better drained sites with feathermoss cover and (b) poorly drained sites with sphagnum cover. Data are from supplementary Table 1 and from Veldhuis (BOREAS Soilsone) and Trumbore (BOREAS TGB12). Carbon is enriched in peaty layers above mineral soil in poorly drained soils.

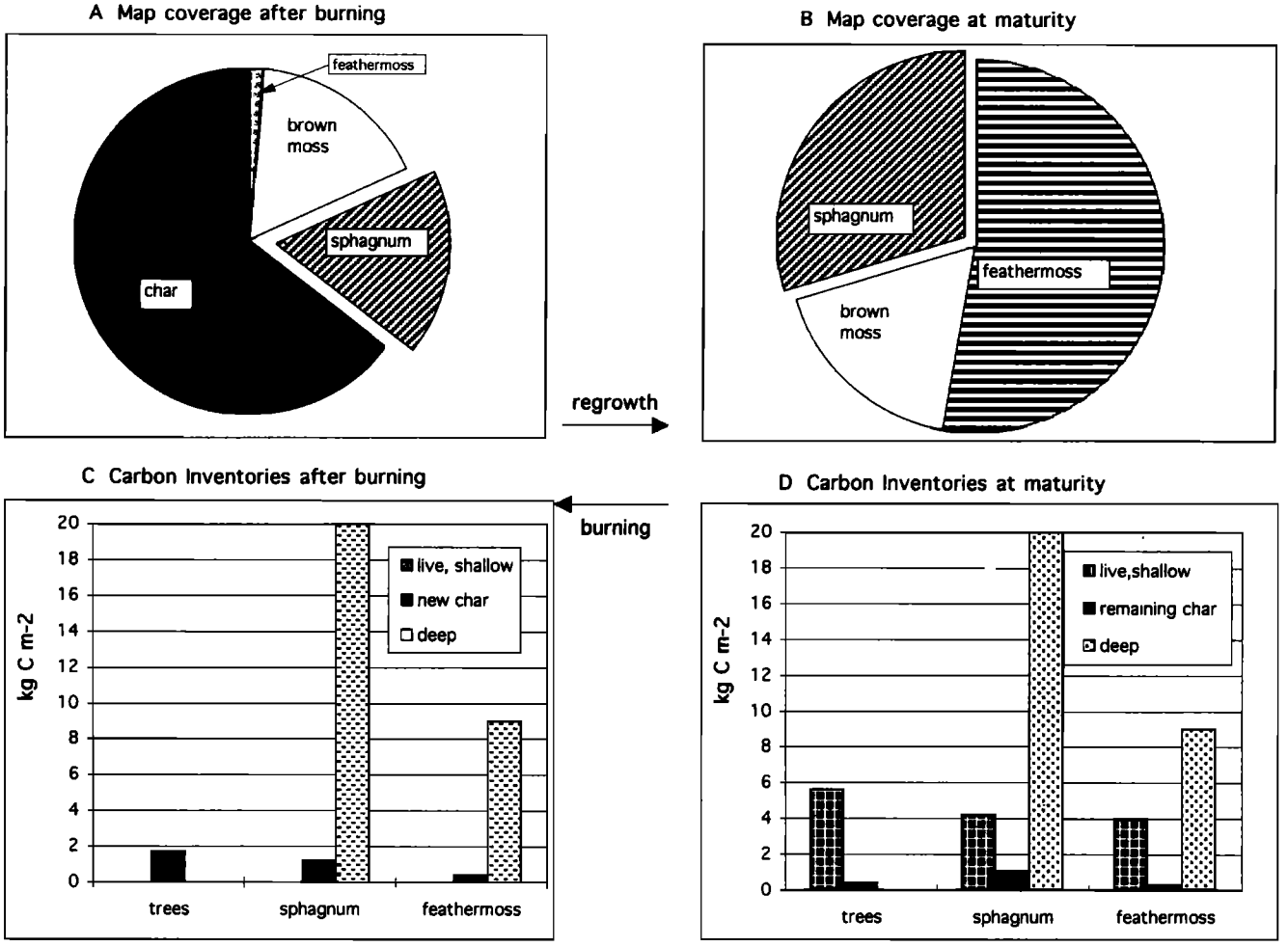

Figure 5. (a, b) Vegetative coverage of moss types according to soil drainage classes in recently burned scenarios (sphagnum cover burns to 25% of imperfect to poorly drained soils; feathermoss burns to 3% of moderately well drained soils; brown moss remains in 17% of area) and mature forest scenarios found at NSA-OBS site today (53% feathermoss on moderately well and half of imperfect to poorly drained soils; 34% sphagnum on half of imperfect to poorly drained and poor to very poorly drained soils; 17% brown moss on very poorly drained and half of very poor to poorly drained soils). (c, d) One-dimensional diagram of carbon inventories in live trees and shallow mosses; charred remains of trees and mosses, and deep organic and mineral soil horizons for recently burned and mature forest stands typical of NSA-OBS. Burn and regrowth arrows indicate changes in carbon inventories modeled after fire transects and soil drainage mapping at OBS; new char in recent burn is based on field inventories of dead trees on recent burn scars and inference of similar burning in mosses. New char in mature stands is based on "deep" decomposition of that char after 117 years of regrowth at OBS, as indicated in Table 3.

time^{-1} (year^{-1}). Resulting data for input and decomposition are presented in Table 3 based on [*Trumbore and Harden*, this issue].

Because decomposition is most likely not constant over time, we also considered models using the equation after *Frolking et al.* [1996]:

$$dC/dt = I/(1 + kt) \tag{3}$$

$$Ct = I/k \ln (1 + kt) \tag{4}$$

This approach assumes that decomposition rates decline over time as the substrate becomes more recalcitrant; the decline is estimated to be linear in proportion to time. However, because differences resulting from these two approaches were not evident over the time span required for this analysis, we employed the simpler of the two models (equations (1) and (2)).

Regrowth and lateral expansion of feathermoss following fire was modeled as a simple linear increase with time:

$$dA/dt = A_0 + A_t * t \tag{5}$$

where A is the area (m^2) covered by feathermoss, A_0 is the percent coverage at time zero (the year of the fire), and A_t represents the incremental area covered by feathermoss each year, as defined by the slope of the percent area versus time curve. For moderately well drained soils and portions of poorly drained soils, we used an A_0 of 3% based on feathermoss occurrence on recent burns. We derived A_t from a linear extrapolation between A_0 of 3% and $A(t)$ at 117 years as estimated for the OBS map. $A(t)$ for feathermoss at OBS, or percent moss cover, could vary anywhere from about 30–53% depending on the ratio of feathermoss to sphagnum in the

Table 1. Carbon Storage in Moss and Soil Layers From a Sequence of Burns in the Northern Study Area

	(FW) 1992 Burn Carbon, kg C m^{-2}	(FF, FFJ) 1989 Burn Carbon, kg C m^{-2}	(GR, GRMJ) 1964 Burn Carbon, kg C m^{-2}	(SOBA, SOAB) 1956 Burn Carbon, kg C m^{-2}	(Setting Lake) 1937 Burn Carbon, kg C m^{-2}	(GRC) 1906 Burn Carbon, kg C m^{-2}	(OBS, OBSP) 1877 Burn Carbon, kg C m^{-2}
			Feathermoss Cover				
Postburn moss, mean	0.00	0.03	0.955	2.26	3.92	...	4.19
Standard deviation >	0.00	0.08	0.926	1.22	3.61	...	1.96
Number (n)	6	7	2	6	2	...	4
Preburn mean	17.20	10.06	12.65	9.37	...	10.90	9.02
Standard deviation	3.54	4.54	4.74	0.25	...	...	1.87
Number (n)	2	2	3	3	...	1	4
			Sphagnum Cover				
Postburn moss, mean>	0.00	0.00	2.03	1.59	2.79	...	4.54
Standard deviation >	0.00	0.00	0.59	0.52	...	...	1.33
Number (n)	4	3	3	2	1.00	...	4
Preburn, mean	...	17.2	16.82	7.22	...	20.4	20.08
Standard deviation	...	...	0.21	...	...	...	4.80
Number (n)	...	1	2	1	...	1	5

Samples were collected by soil horizons above and below recent char layers for sites along 500 m transects. Carbon storage was summed for layers above (postburn) and below (preburn) char layers. OBS,OBSP also includes profiles from H. Veldhuis (personal communication, 1995).

poorly and imperfectly drained soils, so it is also possible that the areal coverage of feathermoss reaches a steady state of about 30% some 50 years after the burn. The sensitivity of our models to this uncertainty is discussed below in the sensitivity analysis section.

The total mass of carbon accumulating on feathermoss sites was modeled as a combination of upward accumulation (thickening) and areal expansion by multiplying (1) and (5). Thus total mass of carbon is a sum of moss accumulation for each areal increment that begins growth at year zero:

$$C_t(t) = \Sigma_0^t A_t(t) * C_t(t - t_0) \quad (6)$$

where $A_t(t)$ is the incremental area that began growth each year starting at t_0, and $C_t(t - t_0)$ is the mass of carbon at age $(t - t_0)$. Net annual flux was then calculated as the difference in carbon storage each year.

Feathermoss contributes dynamic changes in carbon storage over time because of both the areal coverage (Figure 5) and moss-layer thickening (Table 1, Figure 6 transect data). Net primary production estimates (Table 3) from field data (Table 1) fit to (1) are comparable to those of sphagnum moss and much lower than for brown moss, but the rapid decomposition in these well-aerated mosses offsets the production to moderate rates of accumulation (Table 3).

As a check on the model estimates using (1)–(6), we plotted carbon storage of shallow moss for each burn transect (Table 1) against the age of the burn and compared the plot to the model estimates (Figure 6). Several scenarios were used to model the shallow feathermoss accumulation based on the uncertainty in input and decomposition rates (Table 3) and on uncertainties in rates of lateral spread for moss (discussed above). It is clear from the tapering off of the accumulation over time that feathermoss is best modeled as spreading laterally for about 60 years, at which time no significant new areas are colonized by these mosses. Models that allow continued spread of moss after 60 years of regrowth show a much sharper increase in accumulation than was seen in field data. It is also apparent from Figure 6 that the model scenario with high inputs and fast decomposition rates (based on data summarized in Table 3) best fit the observed field data.

C dynamics in sphagnum moss covers. Sphagnum covers about 50–70% of the imperfectly to poorly drained areas as shared by feathermosses and 50% of the poorly to very poorly drained areas as shared by brown mosses. Sites covered by sphagnum mosses tend to dry out in the uppermost layers but remain wet in the deeper organic layers that overlie the mineral soil (Figure 3b). This moisture at depth ensures that mature sphagnum sites do not generally burn down to the mineral soil; consequently, layers of organic material (10–20 cm thick) may be found below recognizable burn layers (Figures 3 and 4). This increase in moisture content with depth also enhances carbon accumulation because decomposition in these lower layers may be anaerobic for at least part of the year. In addition, humic mats under large sphagnum hummocks were often found frozen late into the summer. Bog veneers, however, may burn more completely, as evidenced by the lack of organic horizons below postburn moss in several localities (Figure 1; see also TGB-12 Veldhuis soil maps on WWW).

The occurrence of sphagnum is controlled both by the soil drainage class and by the time since the last fire. This moss favors poorly drained areas, but in the case of bog venees, sphagnum creeps onto better drained areas and creates locally wetter conditions. Sites classified as poor to very poorly drained (Figure 1) are dominated by sphagnum and "wet" mosses, such as "brown" mosses found in rich fens (e.g., *Tomenthypnum nitens*, *Drepanocladus* spp., *Scorpidium scorpioides*, and other members of the *Amblystegiaceae* family); hummocks are most abundant in the flattest or depressional topography (polygons 1, 7, 10, 25, 29 in Figure 1). Deeper organic horizons below the postburn moss were thickest in these soils (total thickness of >40 cm, Figure 1). On sites classified as imperfectly to poorly drained soils (e.g., map units 8, 22, 12), sphagnum is present in mixtures with other mosses: feathermoss tends to dominate the ground cover over drier areas; sphagnum in these polygons occurs either as tussocks or as bog veneers, the latter of which have little or no thick peaty layer underlying the fibric moss layers. These bog veneers appear to have grown upslope and outward from poorly drained, level to depressional sites and from well-established tussocks that retain moisture (Figure 3). The total thickness of

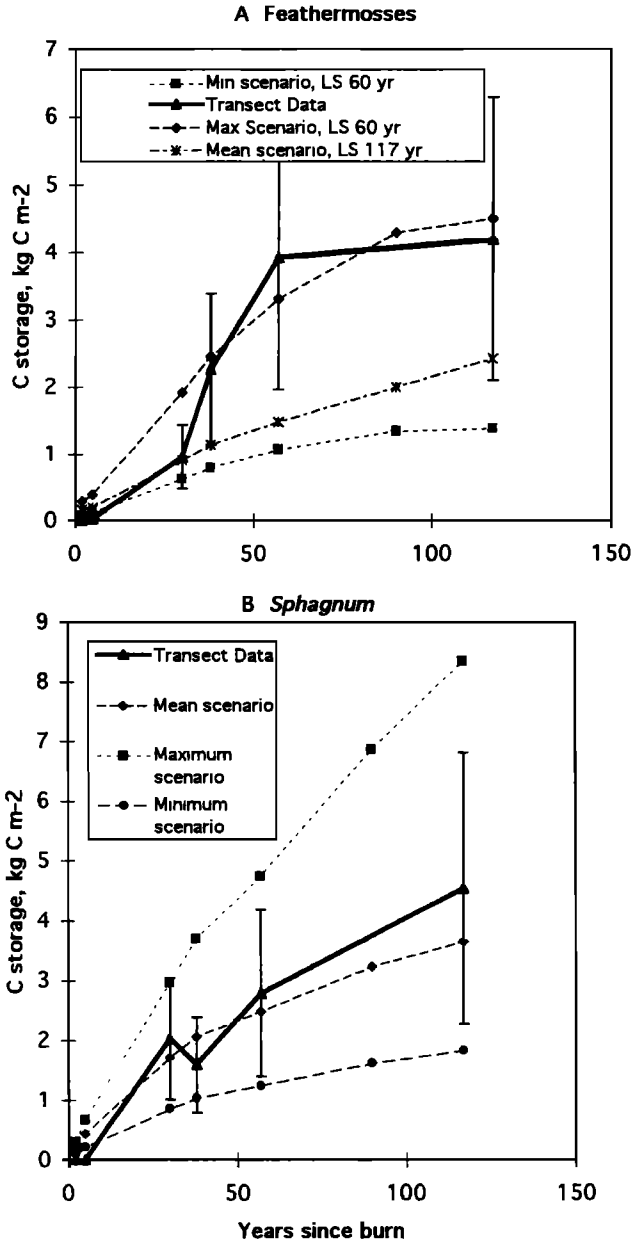

Figure 6. A comparison of shallow moss models versus transect data for forests recovering from fire. Carbon accumulation in feathermoss (a) and sphagnum (b) used Table 3 according to scenarios for minimum, maximum flux discussed in text of this paper. Means (points) and standard deviations (error bars) of transect from Table 1. Tests of lateral spread (LS) of feathermoss ending by 60 years or 117 years, as discussed in text.

organics is generally lower in these places than the poor to very poorly drained areas because of the better drainage and more effective burning. As a result, we estimated that about a half of the sphagnum cover in the imperfect to poorly drained soils burned to mineral soil (e.g., was a thin veneer), and the other half was killed in the fire but allowed to regrow upward (e.g., was comprised of tussocks with thicker, wetter peaty layers). Since a third of the area is covered in feathermoss, the sphagnum cover translates to 35% of the imperfect to poorly drained soils regrowing to 70% (see discussion of sensitivity analysis for uncertainties in cover). For a summation of all sphagnum areas of the OBS map, there is a 19% sphagnum coverage immediately after burning (A_0 in (5)) and 40–54% coverage in mature stands, with A_t = 0.2% per year, as illustrated in Figure 5.

For modeling the changes in carbon storage since the last burn 117 years ago, upward accumulation of carbon in sphagnum uses (1) and (2) based on the results of *Trumbore and Harden* [this issue], which are summarized in Table 3 of this paper. Lateral spread of sphagnum is modeled by using (5). Both attributes are combined in (6) to represent vertical and lateral accumulation. C inputs and decomposition for shallow moss of sphagnum sites are similar to those in feathermoss (Table 3).

As a check on the shallow moss model, we compared mean moss carbon storage for each burn transect (Table 1) to model estimates (Figure 6). Using the mean input and decomposition terms for sphagnum (see caption of Figure 6) [see also *Trumbore and Harden*, this issue], the model and field observations agree quite well. Using minimum or maximum scenarios for carbon dynamics led to carbon values just outside of the observation range.

C dynamics of brown mosses and sedges. Brown mosses and sedges occupy the very poorly drained sites that occur as small fens; these areas represent about 15% of the map area (Figure 1). In the OBS site (Figure 1), most of these fens are collapse features caused by permafrost degradation (thermokarsting). These sites likely burn very infrequently and only in the upper few centimeters above the water table. The depth of organics in these fens ranges from 100 to 160 cm; a basal depth and a ^{14}C age within polygon 1 suggested an age of about 700 years for the collapsed fen. Because fen sites at the OBS tower were remote and logistically difficult to sample, we modeled carbon storage in fens using data from a core taken at the tower fen (FT1) site at BOREAS NSA (Table 2). Both fens have high water tables, brown mosses, and sedge in the upper 1–2 m.

On the basis of *Trumbore and Harden* [this issue], vertical carbon accumulation was modeled by using (1) and (2) and data from FT1 to plot cumulative carbon storage versus basal age (Figure 7). This approach was developed by *Clymo* [1965, 1984], who found mixed success depending on peat composition. The carbon inputs (NPP) to these systems are very high compared to other mosses, but the rates of decomposition and the moss volume contributing to the efflux term offset the shallow accumulation in these systems.

We modeled the very poorly drained fens using inputs and decomposition terms from Table 3. The decomposition term was applied to the entire carbon storage term (Table 3). We did not consider changes in lateral spread of these units (A_0 = 15% and A_t = 0 from (3)) because there was no evidence of very recent permafrost collapse.

C dynamics of prefire deep soil carbon. The amount of carbon stored in organic layers below shallow moss is best estimated by soil drainage class. Imperfectly and poorly drained sphagnum sites store significantly more carbon at depth (Figure 4b, about 19 kg C m^{-2}) than better drained, drier sites that are covered by feathermoss (Figure 4a, about 9 kg C m^{-2}). Carbon storage is greatest in the fen sites (Table 2) which are very poorly drained and often permanently saturated.

In order to quantify the influence of input, decomposition, and burning on deep organic horizons, carbon inventory data from deep organic horizons and mineral horizons were plotted

Table 2. Chemical and Physical Analysis of a Frozen Core From the Tower Fen at the BOREAS Northern Study Area

Basal Depth, cm	Description	Gravimetric Moisture: Field Wet Basis	Gravimetric Moisture: Air Dry Oven-Dry Basis	Bulk Density	Air-Dry Basis: %N	Air-Dry Basis: %C	C/N	Delta ^{14}C	Est Age, Years B.P.*
4	assorted brown mosses	85.4%	10.1%	0.033 g cm^{-3}	1.11	40.74	37	119.2	2
8	mosses	87.8%	10.9%	0.027 g cm^{-3}	1.21	37.55	31	143.4	4
12	fine roots, moss	93.5%	10.5%	0.029 g cm^{-3}	1.40	36.66	26	153.1	6
16	fine roots, moss	96.3%	9.3%	0.045 g cm^{-3}	2.13	38.74	18	292.3	14
21	fine roots, moss	92.0%	10.1%	0.077 g cm^{-3}	2.13	38.74		297.1	20
25	sedge, moss, wood, roots	91.4%	10.5%	0.090 g cm^{-3}	2.25	43.70	19	117.6	29
29	sedge, moss, wood, roots	91.4%	9.9%	0.102 g cm^{-3}	2.25	43.70			
36	sedge, moss, wood, roots	91.3%	11.0%	0.096 g cm^{-3}	2.05	43.48	21	3.5	
42	sedge, moss, wood, roots	94.1%	10.4%	0.063 g cm^{-3}	2.05	43.48			
52	more decomposed mosses	90.2%	11.0%	0.104 g cm^{-3}	1.93	44.12	23	−26.1	
62	fine particles	85.4%	10.5%	0.142 g cm^{-3}	1.65	43.69	26	92.7	
69	fine particles	88.1%	11.4%	0.130 g cm^{-3}	2.08	44.23	21	−57.8	400
350									

Asterisk, values in upper 25 cm estimated from matching maximum ^{14}C to 1965 and matching shape of atmospheric ^{14}C enrichment to ^{14}C enrichment of measured moss leaves.

against radiocarbon age (Figure 7) based on data and methods presented by *Trumbore and Harden* [this issue]. We used data from the deep soil layers (equations (1) and (2)) at site OBSP9, which date back to ~2400 years B.P. The input (I) and decomposition rates (Table 3) from this approach are considerably lower than those of the upper profile.

If we assume that the carbon in deep organic and mineral horizons is derived primarily from the carbon that survives burning, we can use the average rate of carbon input to these layers (Table 3) to estimate the proportion of carbon that is not consumed by fire or by decomposition immediately after fire. For both sphagnum and fen sites the inputs for the deep layers are about 30–40% of the shallow carbon storage at maturity (0.027 deep input *100 years/(3 = storage in moss + 5 in trees). This suggests that if fires occur every 100 years, about 70% of the mature trees and shallow moss is consumed by fire (8 − (0.027 kg C m^{-2} yr^{-1} *100 yr)/8. For independent comparison, there was about about 1.2 kg C m^{-2} residing in fire-killed trees at the two recent burns (Figure 2), which represents about 30% of the live trees at OBS today (Figure 2, J. G. Vogel and S. T. Gower, personal communication, 1997), again suggesting that about 30% of a burned stand enters the soil after a fire. Some of this "char" input is decomposed before the next fire (shown as "new char" in Figure 5), and we estimate the flux term by allowing it to decompose in the deep soil layer. Although there is considerable variation in burn yields and stand ages [*Bonan and Hayden*, 1990], it is likely that most of the long-lasting input to the deep soil layers is in the form of burned material. This is supported by microscope examination of the material, which is black and brown and charred to various degrees.

Decomposition rates in the deep section are 30% of the shallow k values (Table 3) for both sphagnum and fen sites. Slower decomposition in the deep layers is likely related to cooler temperatures, resistant substrates [*Hogg et al.*, 1992] and seasonal water saturation. For the fen sites, lower decomposition at depth must also be related to anaerobic conditions.

The moderately well drained feathermoss sites do not contain any organic layers that are datable with ^{14}C or that accumulate with a regular chronology. *Trumbore and Harden* [this issue] estimated deep I and k values for feathermoss sites based on ^{14}C models of upper mosses and on the ^{14}C of soil gases in winter, a time when the shallow soil gas flux is at a minimum (again, see *Trumbore and Harden* [this issue]). Inputs to the deep feathermoss layers are likely 0.009–0.03 (Table 3) [see *Trumbore and Harden*, this issue], and decomposition is estimated as 0.002 (Table 3).

The carbon flux of deep layers is best modeled as an efflux term, in which the inputs occurred initially at the time of the last fire, and decomposition acted on the dead materials at a

Table 3. Input, Decomposition, and Carbon Storage Terms for Each Soil Drainage/Vegetation Class

	Upper Moss and Soil Layers: Input, kg C m^{-2} yr^{-1}	Upper Moss and Soil Layers: Decomposition, $year^{-1}$	Observed[c] C Storage, kg C m^{-2} yr^{-1}	Long-Term Models of Deep Soil Layers[d]: Input, kg C m^{-2} yr^{-1}	Long-Term Models of Deep Soil Layers[d]: Decomposition, $year^{-1}$	Observed Deep C Storage, kg C m^{-2} yr^{-1}
Feather moss > vertical accumulation[a]	0.03–0.09	0.004–0.018				9[c]
vertical and lateral[b]	0.08–0.02	0.013–0.009	2–4	(0.002–0.005)	0.0006–0.006	
Upland sphagnum > vertical accumulation	0.05–0.15	0.004–0.028				20[c]
vertical and lateral	0.06–0.01	0.008–0.004	2–4	0.007–0.033	0.0005–0.002	
Brown moss fen > vertical accumulation	0.2–0.36	0.022–0.032	5.5 est	0.04–0.06	0.0004–0.0005	30

[a]From *Trumbore and Harden* [this issue] using cumulative accumulation over radiocarbon age.
[b]Mean ± standard deviation for best line fit of transcet data to equation 1 using line-fitting algorithms.
[c]Average values at old black spruce tower, from Table 1.
[d]From *Trumbore and Harden* [this issue] using cumulative accumulation over radiocarbon age and other isotope approaches.

rate determined for the deep carbon pools. For sphagnum sites the input term is equal to 70% of 4 kg C m^{-2} (shallow sphagnum, Table 3) and the decomposition term is 0.0008 (Table 3). Right after burning, the deep pool first inherits the input, then loses about half its mass by the time the site matures over 117 years. The rest of the deep carbon pool (19 kg m^{-2}, Table 3) also decomposes at this slow rate. For feathermoss sites, the input term is 70% of 4 kg C m^{-2} (shallow feathermoss, Table 3), which subsequently decomposes along with 9 kg C m^{-2} of deep organic carbon at a rate of 0.002 $year^{-1}$ (Table 3). Again, the deep pools of carbon decline over the fire cycle as do their proportional effluxes. It is important to recognize that this figure is highly variable from site to site and from year to year and that net exchange of carbon must be strongly tied to the effectiveness/intensity of burning and to the stand age.

Combined flux for the area under the OBS tower. The carbon flux model is a combination of areal and vertical changes in moss and soil over time, expressed as (6) above. To apply (6) to the OBS-NSA site, the OBS map was digitized and polygons were grouped into drainage classes shown in Figure 1. Inferring the extent of burning from the fire sequence data, we allowed shallow, postburn moss to change from bare ground to current cover according to increases in percent area found in the fire sequence (data above). For each year, the amount of area subjected to new moss received plant inputs and lost C to decomposition according to terms in Table 3. Sphagnum and feathermoss were modeled separately according to their input and decomposition rates in Table 3 and rates of lateral spread (see text or caption of Figure 8). Deeper organic layers below the accumulating moss received all of their input 117 years ago and were allowed to decompose at rates shown for deep soil in Table 3. Very poorly drained soils with brown mosses were modeled from long-term accumulation curves of carbon and scaled to the map area according to their present coverage.

The general picture of flux after fire (Figure 8) is one of initially small sinks or net losses of carbon followed by increasing rates of accumulation as the forest regrows. Feathermoss areas are net sources of C right after burns because decomposition occurs on bare, charred ground without much input from moss or trees. Greatest net accumulation of carbon occurs about 60 years following burning, mainly because the lateral expansion of feathermoss reaches a peak around that time. Sphagnum areas are net CO_2 sinks throughout the fire cycle.

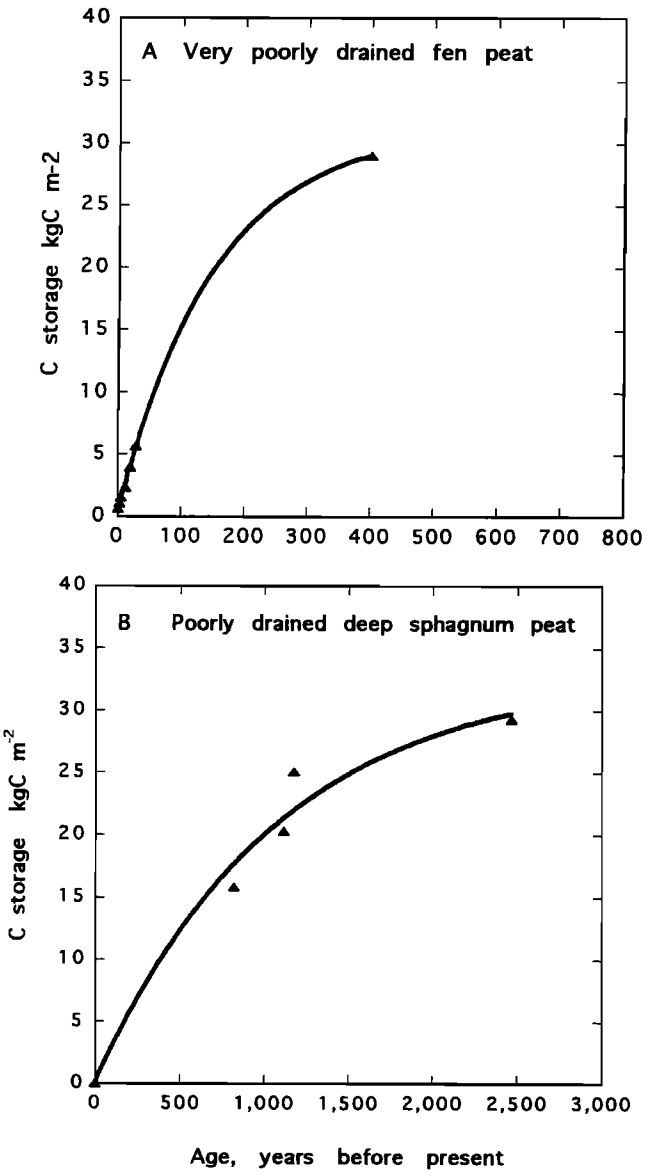

Figure 7. (a) Time plots and curve fits for carbon inventories of A, very poorly drained fen peat and (b) poorly drained, deep sphagnum peat. (a, b) Carbon storage include carbon storage of moss layers based on %C and bulk density measurements; ages are from moss leaves separated and dated from the layers; curve is fit using a line-fitting algorithm for equation (1) to derived input (I) and decomposition (k) values shown in Table 3.

Sensitivity Analysis

The sensitivity of the model to uncertainties in moss cover, carbon storage, and rates of decomposition was evaluated by model iterations. Three factors are especially important to the net flux: percent coverage of regrowing moss, deep carbon stores and the contributing efflux of CO_2, and input and decomposition terms. Rather than construct scenarios to separate how each factor contributes to uncertainties, we combined the information to construct minimum and maximum flux scenarios based on our knowledge of each variable. To minimize carbon sequestration, we (1) maximized areal coverage of sphagnum and its matching deep soil carbon storage because the deep carbon maximizes the efflux contribution, (2) minimized input and maximized decomposition terms (Table 3) but only to the extent that carbon storage at maturity (117 years, age of OBS) was within the observed range (Table 3), (3) maximized deep carbon storage of each moss type (Table 1), which maximizes the deep efflux term, but clearly over the long run, this scenario infers greater net storage. To maximize carbon sequestration we by contrast (1) minimized sphagnum cover to 30%, (2) minimized deep soil carbon storage of sphagnum moss areas, (3) maximized input and minimized decomposition terms for shallow moss within the ranges of Table 3, but again we forced the I and k values to attain a storage term consistent with observed values, (4) minimized deep carbon storage in order to minimize deep efflux. Most notably (Figure 8), both shallow and deep layers may vary by about a factor of 2, but the net exchange varies from about 0.01 to 0.03 kg C m^{-2} yr^{-1} as a net sink of CO_2 to moss and soil. This model does not include the contributions of trees and understory to the net carbon exchange.

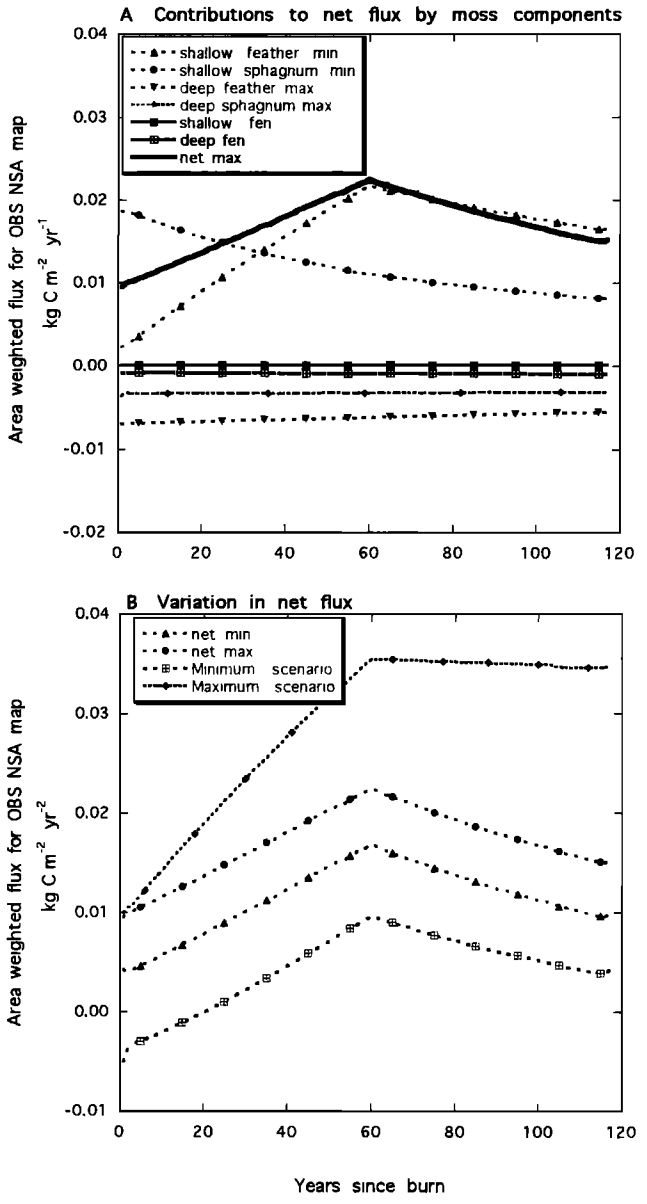

Figure 8. A model of flux contributions from moss and soil to the net carbon exchange of the old black spruce site in Manitoba. The model starts with the OBS area being burned, as illustrated in Figure 4 according to observations on the fire sequence (Figure 2). Percent cover then increases according to equation (5) (see text for values of A_0, A_t), and upward accumulation of growing moss is modeled after equation (2) (Table 3, Figure 7). (a) Contributions by moss components modeled from equations (1)–(6), A_0 feathermoss 2%; A_t feathermoss 0.0033; A_t at 60 yr 40%; deep storage feathermoss 7 kg C m^{-2}; deep k feathermoss 0.002 yr^{-1}; shallow feathermoss I 0.12 kg C m^{-2} yr^{-1}; shallow feathermoss k 0.018 yr^{-1}; A_0 sphagnum 19%; A_t sphagnum 0.002; A_t sphagnum at 117 yr 43%; deep sphagnum storage 15 kg C m^{-2}; deep k sphagnum 0.0005 yr^{-1}; shallow I sphagnum 0.10 kg C m^{-2} yr^{-1}; shallow k sphagnum 0.016; brown-moss I shallow fen 0.213 kg C m^{-2} yr^{-1}; k shallow fen 0.022 yr^{-1}; k deep fen 0.0004; C in shallow fen 9.66 kg C m^{-2}. (b) Net max from Figure 8a; net minimum similar except deep feathermoss k 0.005; deep sphagnum k 0.033; deep fen k 0.0005; minimum scenario uses shallow feather I 0.04 k 0.018; shallow sphagnum I 0.07 k 0.028; deep k same as Figure 8a; maximum scenario uses shallow feather I 0.08, k 0.01; sphagnum I 0.1, k 0.005; deep k same as net maximum.

The model is most sensitive to uncertainties in shallow moss dynamics. Reasons for this uncertainty are based on site variation from which I, k terms were derived [*Trumbore and Harden*, this issue]. The variation in net flux may also involve some bias of near-term measurements of I, k from the past 30 years of ^{14}C accumulation. By contrast, by using the observed carbon storage to constrain the I and k terms, mass balance over the fire may bias model results to the long-term average for I and k. Last, it is likely that a given site fluctuates between high and low flux scenarios because the driving factors of moisture, temperature, and fire vary on an annual to decadal basis. Regardless of these uncertainties, the underlying reality is that these sites, on average, have been and likely continue to be net sinks of carbon. Dramatic or lasting changes in water table or perhaps permafrost would be required to drastically alter the mass balance of flux and storage.

Discussion

To estimate the present-day contributions of CO_2 flux by soil and moss components, the large carbon-storage term of soil (Figure 2) must be modeled over various timescales. Deep carbon changes slowly and over millenia, but because the storage term is so large, it must be included in present-day flux estimates. Shallow mosses, also a large storage term in the boreal forest, can use time sequences of burn scars as surrogates to the decadal timescale. Once we have determined I and k values that can be applied to a variety of organic and mineral soil layers, we can estimate carbon storage and flux for any stand age or soil drainage class if we know (1) the drainage class distribution and (2) the time since the last fire.

Bog veneer and black spruce-moss complexes accumulate carbon in surface mosses and organic soils. Within 117 years of disturbance, mosses in this study sequestered as much or more carbon than trees and 10 times the amount of carbon contained in the understory. Moreover, the rate of carbon accumulation in surface layers probably increases for at least 60 years after burning due to the increasing lateral expansion of mosses (Figure 8). A simple one-dimensional model of soil carbon would not accurately represent carbon storage or flux on annual to decadal timescales, because the thickness of moss varies according to its age since the last fire (areally expanding over time) and because surface mosses are not always indicative of subsurface soils and their carbon content. For example, if one assumes that all of the postburn feathermoss is 117 years old and of the same thickness throughout the tower footprint, the carbon storage of that layer would be 4.5 kg C m^{-2} using I, k of Table 3. By contrast, when the areal growth is used, the carbon storage is 3.5 kg C m^{-2}, a difference of 30%. Although the carbon storage is higher in the first scenario of immediate regeneration, the carbon flux is much more dynamic (and generally higher) in the lateral growth scenario, because some new moss starts growth each year and because rates of C accumulation are highest initially before reaching steady state.

The accumulation of carbon in surface layers is partially offset by the decomposition occurring in deeper layers. Whereas shallow soil layers accumulate over decadal timescales and are best documented for recent fire events, deeper organic layers are inexorably tied not only to current moisture and vegetation but also to those processes, such as fire history, which govern longer-term carbon accumulation in soil. Over millennial timescales, carbon storage in mosses and soils of northern black spruce forests must represent a net CO_2 sink

onto land. The evidence for this sequestration is the accumulation of vast amounts of carbon in poorly drained systems. Our models predict a net accumulation of carbon when shallow inputs exceed shallow and deep decomposition, but inputs and losses from previous burns could conceivably shift the system from sink to source on time intervals of fire cycles. Moreover, periods in which inputs are low and decomposition is high result in small net sources of C from new fire scars (Figure 8b, minimum scenarios). Such scenarios might occur when production is limited by climate, when inputs from burn are low because of severe fire losses, or when decomposition is high. Over time, however, these systems become net sinks of carbon.

Soil drainage is the primary control of carbon accumulation in mosses and organic soils through both ground-moisture effects on fire and effects on decomposition. Carbon dynamics of upland sites (moderately well to poorly drained feathermoss and sphagnum sites) are very similar (Table 3), yet there is a significant twofold difference between deep storage of the poorly drained sphagnum sites to moderately well drained feathermoss sites. Changes in soil drainage resulting from melting or aggradation of permafrost would most likely result in changes in carbon cycling. Although the relative importance of frozen or supersaturated soils have not been addressed by our field studies, it is clear that a warming scenario which induces melting of permafrost could favor carbon sequestration in the poorly or very poorly drained sites, at least temporarily. Warming coupled with lower precipitation, however, would likely result in greater carbon emissions to fire and lower carbon sequestration onto land.

Carbon accumulation calculated using (1) and (2) assumes that the decomposition coefficient is a constant fraction of total carbon throughout the fire cycle. In ecosystems disturbed by fire, however, microbial decomposition may vary with shifts in the soil thermal regime. Microbial respiration is a function of both soil temperature and moisture; as temperatures increase, microbial metabolism increases and respiration rates rise [*Bunnell et al.*, 1977; *Schlenter and Van Cleve*, 1985; *Singh and Gupta*, 1977]. Fire activity may result in a significant increase in soil temperatures. Reduction of leaf area in the canopy and darkening of the forest floor following fire increases solar radiation reaching the forest floor [*Slaughter*, 1983]. Loss of insulating moss and organic horizons results in more rapid transfer of heat from air to ground [*Bonan and Hayden*, 1990]. The combination of these effects results in higher soil temperatures and, when moisture is not limiting or saturating, increased decomposition rates [*O'Neill et al.*, 1996]. As the canopy and moss regrows, increased shading will cool the soil and return decomposition rates to the prefire equilibrium. Under a soil-warming scenario the decomposition coefficient k in (1) would be significantly larger than that predicted for the years immediately following the fire [*Auclair and Carter*, 1993], which may in part explain the "dip" in carbon storage early in the fire sequence (Figure 6). As the soil thermal regime reequilibrates, the value of k will adjust. The long-term effect of increased temperature on carbon storage will depend on the absolute value of the temperature increase and the length of time until soil conditions reequilibrate to prefire conditions. As a first-order estimate of the possible effects of these increased decomposition rates, with a soil temperature increase of 5°C [*Dyrness et al.*, 1986] and a $Q10$ of 2 [*Schimel et al.*, 1994], decomposition rates would be expected to increase by up to 50% in moderately well drained areas that burn. *Auclair and Carter* [1993] estimated that as much as 20% of the carbon stored in the upper meter of soil might be lost to postfire emissions in any given biome. However, wetter, more carbon-rich sites may have lower increases in postfire emissions due to the greater insulating ability of these moss types and the high heat capacity of water [*Trumbore and Harden*, this issue].

At the same time, fire introduces a large pulse of carbon-rich biomass to the soil surface which is variable in its decomposability [*Harmon et al.*, 1990]. Additionally, warmer soils may favor rapid colonization by pioneer species and enhanced growth rates for young plants. Both of these processes will tend to increase carbon inputs to the soil system, offsetting some of the increases in microbial decomposition. Carbon inventories in soils of this study do not show significant evidence of carbon loss after fire, rather the general trend is an increase in storage. Therefore initial inputs of carbon to the soil are likely elevated for a period of time following the fire, partially decomposed during recovery, and contributing to the net carbon accumulation over various timescales.

Conclusion

Our best estimates of C flux at the NSA-OBS site are that it is likely storing about 0.01–0.03 kg C m^{-2} yr^{-1}, or 0.5–0.3 TC ha^{-1} yr^{-1}. Direct measurements of NEP in 1994 and 1995 using eddy correlation show no C accumulation and even C loss from the OBS site [*Goulden et al.*, this issue]. Our estimates are decadal averages and thus could be in accord with eddy flux measurements over longer timescales. 1994 was a year of severe drought, and 1995 of a warm winter in the NSA; both of these conditions would favor low C storage or high C loss through decomposition.

The contributions of moss and soil to the net carbon balance must be discerned from a variety of spatial and temporal approaches, because carbon storage and flux are determined by both present-day distributions and climatic conditions (e.g., moss and soil distribution; net primary production as inputs to soil and moss) and by historic distributions and conditions (e.g., fire history; deeper soil decomposition rates). On the basis of a variety of databases it is clear that over the past century the OBS-NSA site was a net sink of CO_2.

The implications of this approach are that (1) soil drainage controls carbon through habitat for different species, decomposition, and effectiveness of burning, (2) spatial extrapolations must include stand age and associations of soil and moss cover for estimating flux, (3) landform age as well as more recent stand age likely determine how large or small the flux term is from soil layers.

Acknowledgments. Many thanks to John Mason and Gary Hartley for data on forest biomass, Molly Bentley and Carey Masiello for field assistance, and Steve Frolking for help with modeling approaches. Tom Black designed the freeze core for the fens, under a special grant from USGS Global Change funds. Jill Bubier helped with interpretation of the moss types and microclimates. Richard Zepp and Rob Streigl were very helpful in their reviews of an early manuscript.

References

Auclair, A. N. D., and T. B. Carter, Forest wildfires as a recent source of CO_2 at northern latitudes, *Can. J. For. Res.*, *23*, 1530–1536, 1993.

Beltrami, H., and J.-C. Mareschal, Recent warming in eastern Canada inferred from geothermal measurements, *Geophys. Res. Lett.*, *18*(4), 605–608, 1991.

Billings, W. D., Carbon balance of Alaskan tundra and taiga ecosystems: Past, present, and future, *Quat Sci Rev.*, *6*, 165–177, 1987.

Bonan, G. B., and E. S. I. Chapin, Boreal forest and tundra ecosystems as components of the climate system, *Clim Change*, *29*, 145–167, 1995.

Bonan, G. B., and B. P. Hayden, Using a forest stand simulation model to examine the ecological and climatic significance of the late-Quaternay pine-spruce pollen zone in eastern Virginia, U.S.A., *Quat. Res.*, *33*, 204–218, 1990.

Bonan, G. B., D. Pollard, and S. L. Thompson, Effects of boreal forest vegetation on global climate, *Science*, *359*, 717–721, 1992.

Brown, R. J. E., *Effects of Fire on the Permafrost Ground Thermal Regime.*, John Wiley, New York, 1983.

Bunnell, F. L., D. E. N. Tait, P. W. Flanagan, and K. Van Cleve, Microbial respiration and substrate weight loss, I, *Soil Biol. Biochem.*, *9*, 33–40, 1977.

Ciais, P., P. P. Ans, M. Trolier, J. W. C. White, and R. J. Francey, A large northern hemisphere terrestrial CO_2 sink indicated by the 13C/12C ratio of atmospheric CO_2, *Science*, *269*, 1098–1102, 1995.

Clymo, R. S., Experiments on breakdown of Sphagnum in two bogs, *J. Ecol.*, *53*, 747–757, 1965.

Clymo, R. S., The limits to peat bog growth, *Philos. Trans. R. Soc. London*, *303*, 605–654, 1984

Dyrness, C. T., L. A. Viereck, and K. Van Cleve, *Fire in Taiga Communities of Interior Alaska*, Springer-Verlag, New York, 1986.

Francey, R. J., P. P. Tans, C. E. Allison, I. G. Enting, J. W. C. White, and M. Troller, Changes in oceanic and terrestrial carbon uptake since 1992, *Nature*, *373*(26), 326–330, 1995.

Frolking, S., et al., Temporal variability in the carbon balance of a spruce/moss boreal forest, *Global Change Biol.*, *2*, 343–366, 1996.

Goulden, M. L., B. C. Daube, S.-M. Fan, D. J. Sutton, A. Bazzaz, J. W. Munger, and S. C. Wofsy, Physiological responses of a black spruce forest to weather, *J. Geophys. Res.*, this issue.

Harden, J. W., E. T. Sundquist, R. F. Stallard, and R. K. Mark, Dynamics of soil carbon during deglaciation of the Laurentide Ice Sheet, *Science*, *258*, 1921–1924, 1992.

Harmon, M. E., W. K. Ferrel, and F. F. Franklin, Effects on carbon storage of conversion of old-growth forests to young forests, *Science*, *247*, 699–702, 1990.

Hogg, E. H., V. J. Liefers, R. W. Wein, Potential carbon losses from peat profiles: Effects of temperature, drought cycles, and fire, *Ecol. Appl.*, *2*(3), 2298–306, 1992.

Houghton, R. A., Is carbon accumulating in the northern temperate zone?, *Global Biogeochem. Cycles*, *7*(3), 611–617, 1993.

Lachenbruch, A. H., Permafrost, the active layer, and changing climate, U.S. *Open File Rep. 94-694*, U.S. Geol. Surv., Washington, D. C., 1994.

O'Neill, K. P., S. Kasischke, and D. D. Richter, The effect of fire on biogenic carbon emissions from soils of interior Alaska, *Eos Trans. AGU*, *77*(46), Fall. Meet., Suppl., F185, 1996.

O'Neill, K. P., J. W. Harden, S. E. Trumbore, M. O. Bentley, G. W. Winston, and B. B. Stephens, Boreal-Ecosystem Atmosphere Study (BOREAS): 1993 site descriptions and field notes, *U.S Geol. Surv Open File Rep. 95-488*, in press, 1997a.

O'Neill, K. P., J. W. Harden, and S. E. Trumbore, Boreal-Ecosystem-Atmosphere Study (BOREAS): 1993 laboratory data and notes, Thompson, Manitoba, *U.S Geol. Surv. Open File Rep. 95-565*, in press, 1997b.

Racine, C. H., Tundra fire effects on soils and three plant communities along a hill-slope gradient in the Seward Peninsula, Alaska, *Arctic*, *34*(1), 71–84, 1981.

Schimel, D. S., B. H. Braswell, E. A. Holland, R. McKeown, D. S. Ojima, T. H. Pinter, W. J. Parton, and A. R. Townsend, Climatic, edaphic, and biotic controls over storage and turnover of carbon in soils, *Global Biogeochem Cycles*, *8*(3), 279–294, 1994.

Schlenter, R. E., and K. Van Cleve, Relationships between CO_2 evolution from soil, substrate, temperature, and moisture in four mature forest types in interior Alaska, *Can. J. For. Res.*, *15*, 97–106, 1985.

Singh, J. S., and S. R. Gupta, Plant decomposition and soil respiration in terrestrial ecosystems, *Bot. Rev.*, *43*, 449–528, 1977.

Slaughter, C. W., Summer shortwave radiation at a subarctic forest site, *Can. J. For. Res.*, *13*, 740–746, 1983.

Stocks, B. J., Black spruce crown fuel weights in Ontario, *Can. J For. Res.*, *10*, 498–501, 1980.

Stocks, B. J., Fire behavior in mature jack pine, *Can. J. For. Res.*, *19*, 783–799, 1989.

Tans, P. P., I. Y. Fung, and T. Takahashi, Observational constraints on the global atmospheric CO_2 budget, *Science*, *247*, 1431–1438, 1990.

Thie, J., Distribution and thawing of permafrost in the southern part of the discontinuous permafrost zone in Manitoba, *Arctic*, *27*, 189–200, 1974.

Trumbore, S. E., and J. W. Harden, Accumulation and turnover of carbon in organic and mineral soils of the BOREAS northern study area, *J. Geophys Res.*, this issue.

Walker, J. D., and B. J. Stocks, The fuel complex of mature and immature jack pine stands in Ontario, *Inf. Rep. O-X-229*, 19 pp., Dep. Environ. Can. For. Serv., Sault Ste. Marie, Ontario, Can., 1975.

Zoltai, S. C., Cyclic development of permafrost in the peatlands of northwestern Alberta, Canada, *Arc. Alp Res.*, *25*, 240–246, 1993.

J. W. Harden and K. P. O'Neill, U.S. Geological Survey, 345 Middlefield Rd., Menlo Park, CA 94025. (e-mail: jharden@usgs.gov)

B. J. Stocks, Forestry Canada, Sault Ste. Marie, Ontario, Canada.

S. E. Trumbore, Earth System Science, University of California, Irvine, CA 92717

H. Veldhuis, Agriculture Canada, Winnipeg, Manitoba.

(Received April 26, 1996; revised June 26, 1997;
accepted June 26, 1997.)